Elham ABDULLAH[1]*,
Abdulkareem JALIL[1]

ENHANCING EXPERIMENTAL PREDICTION OF SPRINGBACK IN FORMING PROCESSES USING ADVANCED FINITE ELEMENT MODELLING

The springback phenomenon (SBP) is a prevalent, costly, and challenging problem. It occurs in metals during sheet metal forming processes (SMFPs). Experimental studies can contribute to significant errors that prevent the target data acquisition. Accordingly, this research aims to bridge this gap by choosing other inspection approaches, reflected in finite element analysis (FEA) and machine learning (ML) integration, to forecast probable issues of SBP in heavily utilized metals across diverse manufacturing domains, namely 99% pure aluminum, 99% pure copper, and low-carbon steel. Material deformation, peak forming force, equivalent Von Mises stress distribution, and thermal effects are examined under different thicknesses and punch radii. ANSYS simulation results show that 99% pure aluminum has the highest springback (6.2%) due to its ductility, followed by 99% pure copper (4.0%) and low-carbon steel (2.5%), which has superior dimensional stability. The forming force requirements were lowest for 99% pure aluminum (50 kN), moderate for 99% pure copper (75 kN), and highest for low-carbon steel (100 kN). 99% pure copper had the highest temperature rise (350°C), while low-carbon steel had the highest Von Mises stress (420 MPa), demonstrating its strength but vulnerability to localized stress. The hybrid FEA-ML model has effectively and accurately predicted springback angles. The results also show that 99% pure aluminium is best for lightweight structures, low-carbon steel for strength-critical designs, and 99% pure copper for high ductility needs.

1. INTRODUCTION

Springback is a key metal forming process where materials undergo elastic recovery following plastic deformation, generating dimensional inaccuracies in the final product. This is especially troubling in industries like automotive, aerospace, and manufacturing, which require 99% pure aluminium, 99% pure copper, and low-carbon steel. The specific mechanical properties of these materials determine their springback behaviour. 99% pure aluminium has low yield strength and high ductility, causing springback in bending and deep drawing. 99% pure copper has a higher yield strength and work hardening than 99% pure aluminium, hence it has different springback qualities. Low-carbon steel has less springback because to its higher strength and lower ductility, although predictions are difficult. So, to

_____
[1] Department of Mechanical Engineering, College of Engineering, University of Babylon, Babylon 51001, Iraq
* E-mail: huda24576@gmail.com
  https://10.36897/jme/202916

improve process efficiency, reduce material waste, and ensure dimensional correctness in metal forming, springback must be known and predicted.

Analytical and empirical models are the main methods for forecasting springback, using simplified approximations of material behaviour and process circumstances. These models are useful for fundamental applications, but they often overlook the intricacies of real-world forming processes. 99% pure aluminium, 99% pure copper, and low-carbon steel show nonlinear, time-dependent deformation behaviour, making it hard for standard models to forecast springback across process conditions. These models generally can't include material anisotropy, effective strain rate sensitivity, and temperature effects, which all greatly affect springback in real-world applications. These limits show the need for more advanced methods that can capture the complex interactions between material properties, forming circumstances, and springback behaviour.

Finite Element Analysis (FEA) is a common method for simulating metal forming processes like springback prediction. FEA models material deformation in depth, including plasticity, effective strain rate sensitivity, and material anisotropy. Many studies show that FEA can consistently forecast springback with the correct material models, boundary conditions, and mesh upgrades. Despite its accuracy, FEA is computationally expensive, particularly when working with sophisticated geometries, enormous datasets, or parametric research. This computing cost renders FEA inappropriate for firms that need rapid and frequent design iterations or optimisation involving several process components. To fix FEA's flaws, ML approaches have become a more effective springback prediction solution [1]. Supervised learning techniques in machine learning can capture the complicated, nonlinear linkages between process parameters, material properties, and springback behaviour without requiring explicit physical models [2]. ML's springback prediction use has been studied. Bolar et al. [3] created an artificial neural network (ANN) model to forecast springback in V-bending procedures for 99% pure aluminium. Their findings demonstrated that ANNs could predict springback by learning from process characteristics including punch speed, sheet thickness, and material hardness. Wang et al. [4] also used SVM to predict springback in copper sheet metal forming, showing that SVM models can generalise across forming conditions and material factors, yielding accurate predictions with less computational effort than FEA.

Machine learning models need lots of training data, which might come from physical experiments or simulations [5]. This has caused FEA and machine learning hybrid models. Machine learning algorithms can be trained to provide quick predictions without full FEA simulations for each design iteration by utilising FEA to produce massive datasets of simulation results under different process conditions and material attributes [6]. He et al. [7] devised a hybrid model that combines FEA and Support Vector Regression (SVR) to anticipate springback in 99% pure aluminium sheet metal forming. The model, trained on FEA simulation data, predicts better and computes faster than normal FEA. Zeinolabedin-Beygi et al. [8] estimated springback in 99% pure copper and low-carbon steel forging with FEA and Random Forest models. The hybrid model cut springback prediction time by 60% and retained accuracy.

The hybrid method is great for optimising metal forming. Machine learning and FEA simulations can better predict how die shape, material thickness, punch speed, and

temperature affect springback behaviour [9, 10]. This technology also allows for faster and more efficient design optimisation, since machine learning algorithms can quickly predict various scenarios, reducing the need for extensive simulations or physical trials [11]. Hybrid models can be adapted for diverse metals, including 99% pure aluminium, 99% pure copper, and low-carbon steel, each of which requires numerous material models to depict its specific springback behaviour [12] properly.

In summary, springback prediction is still a major problem in metal forming processes, which have unique mechanical properties and deformation behaviours. FEA is fantastic for mimicking springback, but its computing cost limits its utility in real-time design optimisation and iterative testing. Machine learning is a useful alternative since it learns difficult relationships from data, allowing for speedier predictions without thorough physical models. When combined with FEA, machine learning may greatly enhance the accuracy, efficiency, and scalability of springback predictions, providing a hybrid solution that benefits companies where speed, precision, and cost-efficiency are vital. So, FEA and machine learning may fix springback difficulties and improve metal forming in 99% pure aluminium, 99% pure copper, and low-carbon steel.

This study proposes a hybrid analysis that combines machine learning's predictive power with FEA's exact simulations. The goal is to build a robust machine learning model that can accurately predict springback in metals, especially 99% pure aluminium, 99% pure copper, and low-carbon steel, using FEA-generated data. This method uses supervised learning algorithms and FEA simulations to enhance springback angle predictions, minimise trial time, and optimise metal forming. The proposed hybrid approach may help firms who need to control material behaviour during forming processes, improving product quality and manufacturing efficiency.

2. MATERIALS AND METHODS

In this study, three common metals utilized in manufacturing, namely 99% pure aluminum, 99% pure copper, and low-carbon steel, are considered for SBP prediction in SMFPs. These metals were selected due to their distinct mechanical properties, which influence their springback behaviour and are widely used in industries such as automotive, aerospace, and manufacturing. 99% pure aluminum is a light, ductile metal with relatively low yield strength and high workability, which makes it prone to springback, particularly in processes like bending and deep drawing. The material is frequently used in aerospace and automotive applications where weight reduction is a priority [13, 14]. 99% pure copper is a highly ductile material with excellent thermal and electrical conductivity. It has a higher yield strength compared to 99% pure aluminum, which results in different springback characteristics. 99% pure copper is commonly used in electrical components and plumbing systems [15]. Low-carbon steel, specifically in its commercial form as mild steel, is stronger but less ductile compared to 99% pure aluminum and 99% pure copper. It is commonly used in structural and automotive components. Its springback behaviour is influenced by its relatively higher yield strength and lower ductility [16].

The mechanical properties of these metals, including Young's modulus, yield strength, Poisson's ratio, and effective strain-hardening behaviour, were considered when developing the material models for the simulations. These properties were extracted from standard material databases and experimental data.

2.1. FINITE ELEMENT ANALYSIS (FEA) SIMULATIONS

FEA simulates the SMFPs and SBP predictions for the three metals in the ANSYS software package, a widely used simulation software. FEA is employed to model the forming processes, predict deformation, and evaluate the resulting springback behaviour under varying conditions [17].

Springback in metals expresses the elastic recovery that occurs after unloading in SMF processes. To estimate springback by the ANSYS Workbench, the main problem of springback should be identified. Also, material properties should be carefully chosen. The geometry should be set up. Additionally, appropriate boundary conditions that simulate the sheet metal forming, unloading process, and springback should be recognized and chosen.

The most important procedure is to choose the right ANSYS solver for this problem, which is the ANSYS Workbench (Mechanical), specifically Explicit Dynamics (LS-DYNA), which is formulated to analyze high-strain rate processes and static structural loading connected to slow deformations and stress and strain under very low speeds or static conditions. LS-DYNA ANSYS package can uncover critical metal properties, including yield stress, Von Mises stress, elastic strain, and deformations.

The metal forming process was modelled as a simple V-bending operation to study the SBP. A V-die was used with a punch, where the material was subjected to bending at various punch speeds and sheet thicknesses to investigate the effects of these parameters on SBP. The metal models used in FEA were chosen to reflect the mechanical properties of 99% pure aluminum, 99% pure copper, and low-carbon steel. For each material, an appropriate plasticity model, such as the isotropic or kinematic hardening models, was employed to simulate the nonlinear behaviour under forming conditions [18]. The Johnson-Cook material model was utilized for 99% pure copper and low-carbon steel to account for temperature and effective strain rate effects, while for 99% pure aluminum, a Hill48 yield surface was used to capture its anisotropic plastic behaviour. Table 1 illustrates the critical properties of these three metals. Most of these variables and their corresponding values will be exploited to identify the boundary conditions linked to the three explored metals.

The boundary conditions chosen for the simulation included fixing the die at the bottom and applying a displacement-controlled load to the punch to simulate the bending process. The contact between the punch, sheet metal, and die was modelled using frictional contact, with a coefficient of friction set based on typical values for metal forming processes. A fine mesh was applied to the region of interest (the sheet metal and contact surfaces) to ensure accurate results in terms of equivalent Von Mises stress, effective strain, and springback predictions [19, 20]. The meshing procedure is one of the important processes that should be carefully implemented to make sure accurate numerical outcomes and high-quality results are reached. The first step in meshing is to study the structure. Some mechanical difficulties, such

as circular cross-section beams, rectangular parallelepiped mechanical problems, and square-like top and side faces of materials, can be quite simple [21]. In some cases, mechanical structures can be very complex, as they reflect bigger mechanical structures used in real-world production, such as ships, vehicles, or aircraft.

For these complicated structures, adopting simple mathematical models could not offer accurate results because of various defects and inaccuracies while leveraging a single framework that expresses the full vehicle structure of the automobile, ship, or aeroplane. Table 2 illustrates the critical meshing variables and their values used in this simulation study, which include the meshing technique and the overall number of shape elements of the three specimens built in SolidWorks®.

Table 1. Critical common mechanical and physical properties of the three inspected metals

No.	Mechanical and Physical Properties	Metal Name		
		Low-Carbon Steel	99% Pure Aluminum	99% Pure Copper
1	Colour	Gray	Silvery-White	Red-Orange
2	Density	7,850 kg/m^3	2,700 kg/m^3	8,920 kg/m^3
3	Tensile Strength	420 MPa	90 MPa	210 MPa
4	Modulus of Elasticity/ Young's Modulus	200 GPa	68 GPa	120 GPa
5	Shear Modulus	80 GPa	25 GPa	44 Gpa
6	Poisson's Ratio	0.25	0.36	0.35
7	Melting Temperature Point	1,205 °C to 1,370 °C	660 °C	1,083 °C
8	Thermal Conductivity	44 to 52 W/m.K	237 W/m.K	260 W/m.K
9	Vickers Hardness	126 HV	150 to 160 HV	40 to 110 HV

Table 2. Major meshing characteristics of the selected three metals

No.	Category	99% Pure Aluminum	99% Pure Copper	Low-Carbon Steel
1	Type of the Chosen Cell	Hexahedral (for structured meshing)	Tetrahedral (for flexibility in geometry)	Tetrahedral (for flexibility in geometry)
2	Dimensions of the Geometric Shape	200 mm × 100 mm × 2 mm (for sheet metal)	200 mm × 100 mm × 2 mm (for sheet metal)	200 mm × 100 mm × 2 mm (for sheet metal)
3	The Overall Number of Meshing Elements	150,000 - 250,000 elements (depending on mesh refinement)	150,000 - 250,000 elements (depending on mesh refinement)	150,000 - 250,000 elements (depending on mesh refinement)

The mesh was refined in areas with high gradients in equivalent Von Mises stress and effective strain, and an appropriate mesh size was chosen to balance accuracy and computational efficiency [22]. The simulations were run for various process parameters, including different punch speeds (to examine effective strain rate sensitivity) and material thicknesses [23]. Temperature effects were considered in simulations for 99% pure copper

and low-carbon steel due to their high sensitivity to temperature during metal forming processes than 99% pure aluminium.

<div align="center">2.2. MACHINE LEARNING MODEL</div>

A hybrid machine learning approach was employed to develop a predictive model of SBP, combining FEA simulation data with supervised learning algorithms. The primary steps in developing the ML model are as follows:

1. Data Generation: FEA simulations were performed for a range of process parameters, such as punch speed, material thickness, and die geometry. The simulation data, including the springback angles, were collected for each material (99% pure aluminum, 99% pure copper, and low-carbon steel) under different forming conditions [24].

2. Feature Selection: The input features for the ML model included process parameters such as punch speed, sheet thickness, material properties (such as yield strength Young's modulus), and the temperature during forming. These features were chosen based on their known influence on springback behaviour. The target output variable was the springback angle, representing the amount of elastic recovery in the metal after forming [24].

<div align="center">2.3. HYBRID MODEL INTEGRATION</div>

A hybrid model for forecasting springback behaviour in metal forming processes uses FEA and ML [26]. This hybrid method leverages FEA and ML's strengths to improve SBP prediction accuracy and efficiency. This hybrid method was investigated in terms of its methodology, and benefits. The major research methodology, which utilizes the proposed hybrid advanced FEA-ML framework, and its necessary steps can be outlined in Fig. 1.

Data Generation through FEA Simulations
Run FEA simulations for various process parameters, such as punch speed, sheet thickness, and material properties, to generate data on springback angles.

Data Preprocessing and Feature Selection
Process the generated data and select key features, such as material properties and process parameters, that influence springback behavior.

Model Training
Model Training: Use the preprocessed data to train the machine learning SVM model.

Model Testing and Validation
Evaluate the trained model with test data to assess its accuracy and reliability.

Hybrid Model Integration for Real-Time Predictions
Integrate the machine learning model with FEA to predict springback in real-time, enabling faster, more efficient decision-making in metal forming processes
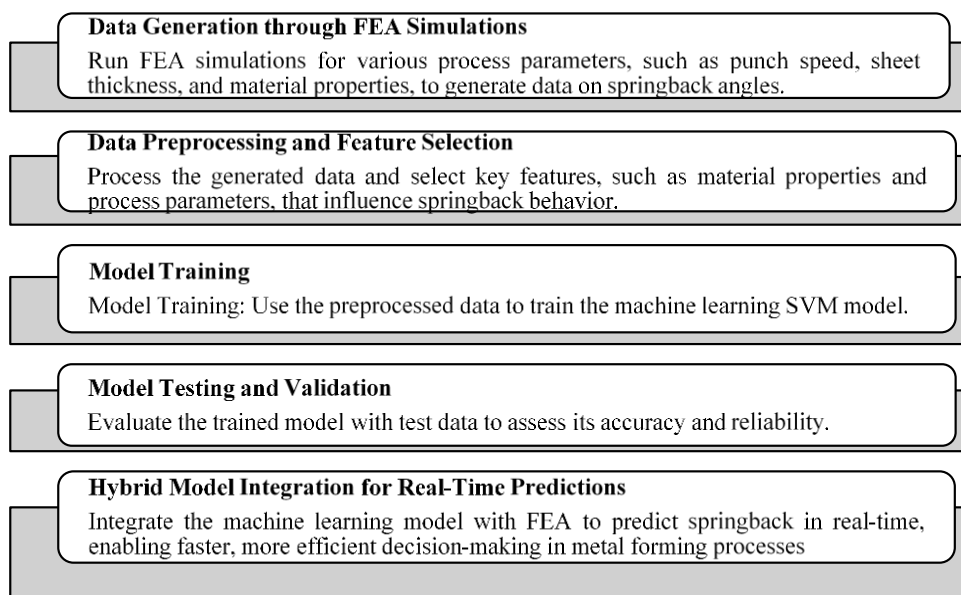
Fig. 1. The proposed research methodology that uses hybrid FEA-ML framework

FEA is useful for modelling complex physical processes in metal forming, like plastic deformation, effective strain-rate sensitivity, and material anisotropy, but it is costly to compute, especially for large-scale or parametric research [4]. These computing constraints limit its real-time application and practicality in industrial settings where quick iterations and optimisation are important. On the other hand, ML, particularly supervised learning algorithms, can offer quick and efficient predictions by learning complex, nonlinear relationships between input parameters (such as material properties and process conditions) and the output (springback) [26]. However, ML models require large datasets for training, which are often not readily available and must be generated via time-consuming physical experiments or FEA simulations. Thus, combining FEA with ML can generate high-fidelity data under various forming conditions, which is then used to train machine learning models [27]. This hybridization capitalizes on the predictive capabilities of ML while maintaining the physical accuracy provided by FEA simulations.

3. MODELS AND DIE MECHANICAL DESIGN

In the proposed simulation process, critical graphical data were obtained, reflecting the mechanical properties of various specimens. Figures 2–4 visually represent the 3D CAD layouts of the 99% pure aluminum, 99% pure copper, and low-carbon steel specimens, respectively, after they were subjected to the die load, causing metal bending.
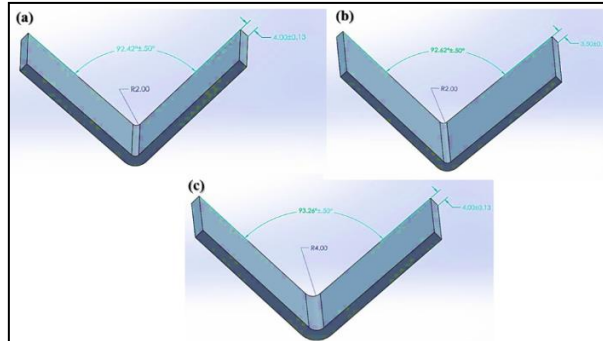

Fig. 2. 3D CAD layouts of the 99% pure aluminum specimens after bending after applying the die load with various thicknesses and punch radiuses
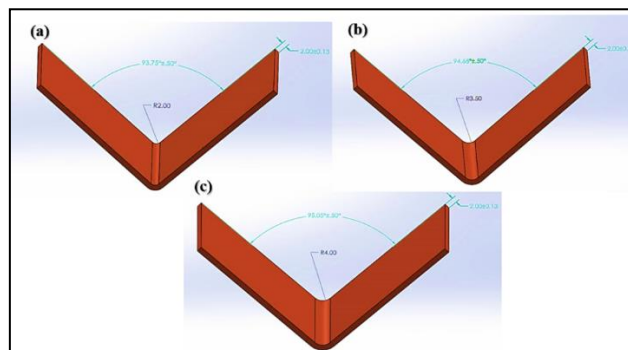

Fig. 3. CAD layouts of 99% pure copper specimens after bending after applying the die load with various thicknesses and punch radiuses
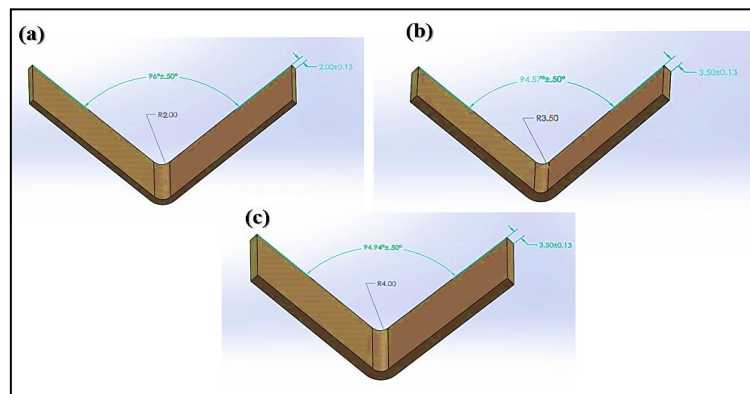
Fig. 4. 3D CAD layouts of low-carbon steel specimens after bending after applying the die load with various thicknesses and punch radiuses

For the 99% pure aluminum specimens, two specimens have a thickness of 4.0 ± 0.13 mm with a punch radius of 2.0 ± 0.13 mm and 4.0 ± 0.13 mm, respectively. While the third aluminum sheet metal sample has a thickness of 3.5 ± 0.13 mm and a punch radius of 2.0 ± 0.13 mm. The first, second, and third aluminum sheet metals have bend angle values of 92.42° ± 0.50°, 92.62° ± 0.50°, and 93.26° ± 0.50°.

Similarly, the three 99% pure copper specimens also have a thickness of 2 ± 0.13 mm. The first, second, and third copper specimens have punch radius amounts of 2.0 mm, 3.5 mm, and 4.0 mm, respectively. Their bending angle rates are, in order, 93.75° ± 0.50°, 94.68° ± 0.50°, and 95.05° ± 0.50°.

For the low carbon steel, the first, second, and third sheet metals have thicknesses of 2.0 ± 0.13 mm, 3.5 ± 0.13 mm, and 3.5 ± 0.13 mm, respectively. Their punch radius amounts are 2.0 mm, 3.5 mm, and 4.0 mm. Their bending angles are, in order, 96.00° ± 0.50°, 94.57° ± 0.50°, and 94.94° ± 0.50°.

Figure 5 shows that the dies are made to apply die loading in the SMFP. Figure 5a shows that the 3D die used in this investigation is V-shaped. Figure 5b and 5c shows the copper specimen's deformations after the force was applied.
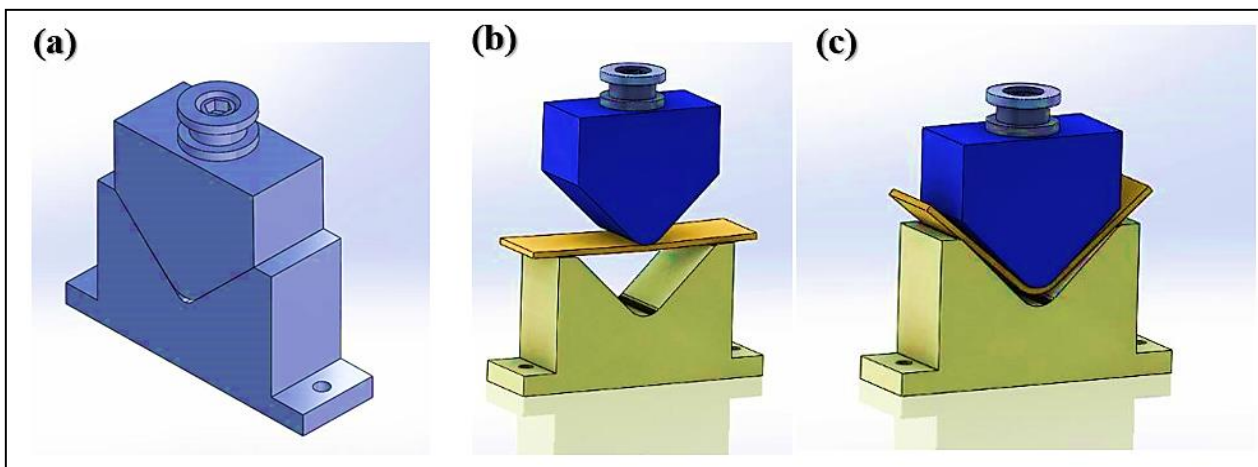

Fig. 5. 3D CAD layouts of (a) the die utilized, (b) a 99% pure copper sheet metal on which the die load is applied, and (c) the deformed 99% pure copper sheet metal after bending

4. FEA RESULTS ANALYSIS

The numerical ANSYS findings also showed certain outcomes for the six specimens (two each of 99% pure aluminium, 99% pure copper, and low-carbon steel). Table 3 shows these results. Graphs were made to show the significance of these results. Figure 6 shows the applied load on the three metals over time, each with two examples. Figure 7 shows the equivalent stress-effective strain profiles of the three metals studied, each with two specimens and load application time.

Table 3. The numerical outcomes of the effective strain analysis of the six samples

Time (Sec's)	Effective Strain Rate (99% Pure Copper Specimen [1])	Effective Strain Rate (99% Pure Copper Specimen [2])	Effective Strain Rate (99% pure Aluminum Specimen [1])	Effective Strain Rate 99% pure Aluminum Specimen [2])	Effective Strain Rate (Low-Carbon Steel Specimen [1])	Effective Strain Rate (Low-Carbon Steel Specimen [2])
0.16	0.06125	0.07250	0.04500	0.05875	0.04000	0.04125
0.24	0.06125	0.07375	0.04375	0.05875	0.04000	0.04125
0.32	0.06125	0.07250	0.04500	0.05875	0.04000	0.04125
0.40	0.06125	0.07250	0.04375	0.06000	0.04000	0.04125
0.48	0.06125	0.07250	0.04500	0.05875	0.04000	0.04125
0.56	0.06125	0.07375	0.04375	0.05875	0.04000	0.04125
0.64	0.06125	0.07250	0.04500	0.05875	0.04000	0.04125
0.72	0.06125	0.07250	0.04375	0.05875	0.04000	0.04125
0.80	0.06125	0.07250	0.04500	0.05875	0.04000	0.04125
0.88	0.06125	0.07250	0.04375	0.05875	0.04000	0.04125
0.96	0.06125	0.07375	0.04500	0.05875	0.04000	0.04125
1.04	0.06125	0.07250	0.04375	0.05875	0.04000	0.04125
1.12	0.06125	0.07250	0.04500	0.05875	0.04000	0.04125
1.20	0.06125	0.07250	0.04375	0.05875	0.04000	0.04125

Figure 6 shows that the second 99% pure copper specimen has the highest effective strain rates (0.073 across the numerically simulated time), followed by the first 99% pure copper specimen (0.062) and the second 99% pure aluminium specimen (0.0585). In contrast, the lowest effective strain rates were found in the first and second low-carbon steel specimens, accounting for 0.040 and 0.041, respectively. The first 99% pure aluminium specimen, which is lighter than low-carbon steel and is remarkably feasible for making light-weight automobiles, has a very close effective strain rate to the two low-carbon steel specimens, whose effective strain rate reached 0.045.

In addition, referring to the numerical simulation results expressed in Table (3), relevant graphical illustrations can be expressed in Fig. 7, which indicates the equivalent stress-effective strain profiles related to the three inspected metals. It can be inferred from this figure that the three metals underwent a special uniform plastic strain phase from initial and final values of the effective strain, corresponding to constant equivalent stress, which was approximately similar to the three metals. It is important to study such effective strain-curve to understand the behaviour of SBP and, thus, optimize their dimensions, properties, and critical variables when these metals are utilized in different manufacturing disciplines.
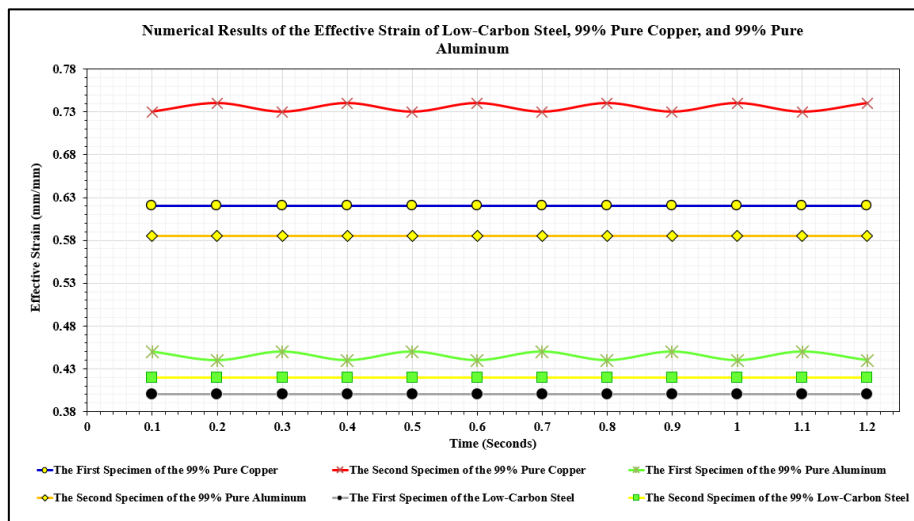
Fig. 6. The effective strain of the three investigated metals varying with time, each with two same specimens
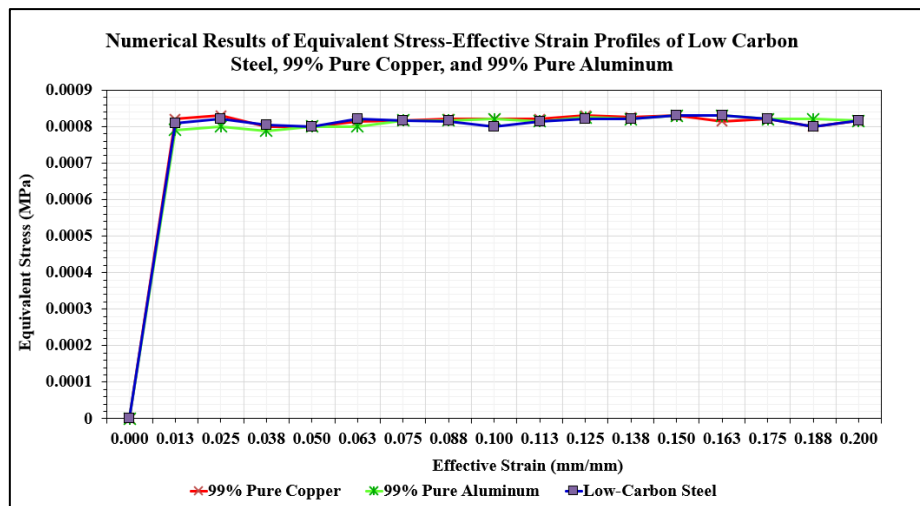

Fig. 7. The equivalent stress-effective strain profiles of the three investigated metals with the load application time, each with two specimens

In addition, Fig. 8 explains the behaviour of the three metals when the die load was applied over a range of time. It can be shown that the three metals followed a constant linear deformation behaviour with time, implying their active response to the load amount with time. As a result, in the manufacturing context, elongations can be continually recorded in such metals with increasing and lengthy implementation of the die load. Therefore, careful observations and control of this process should be ensured to avoid excessive elongations and deformations that may correspond to significant distortions in the metal. Besides, the mathematical simulation findings uncovered some statistical figures on the elastic recovery that occurred in accordance with the SBP in the three investigated metals, 99% pure aluminum, 99% pure copper, and low-carbon steel specimens, each with three thicknesses, i.e., an overall of nine samples were attained for the three metals.

The results indicate that the SBP-related behaviour would increase with the metal dimension (punch radius). Those 99% pure aluminium specimens with lower thicknesses

would have bigger effects and noteworthy SBP consequences compared with aluminium specimens with higher thicknesses. More deformation occurs with thicker metal.
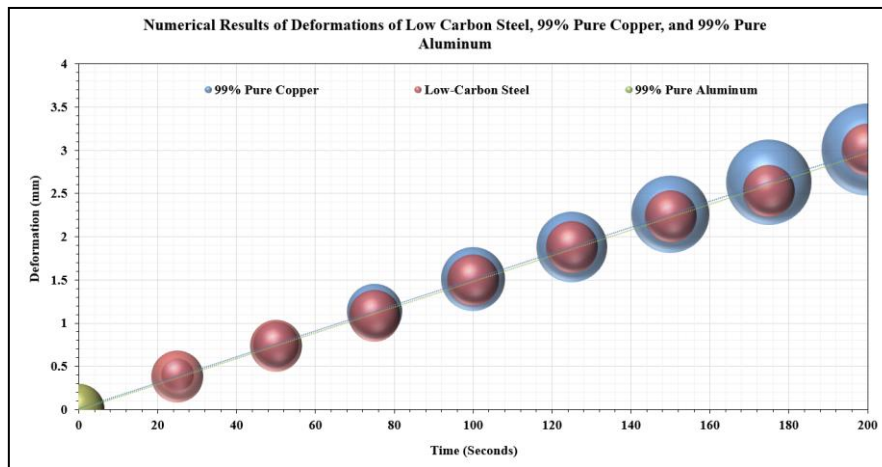

Fig. 8. Numerical simulation outcomes of deformations of the three investigated metals varying with the load application time
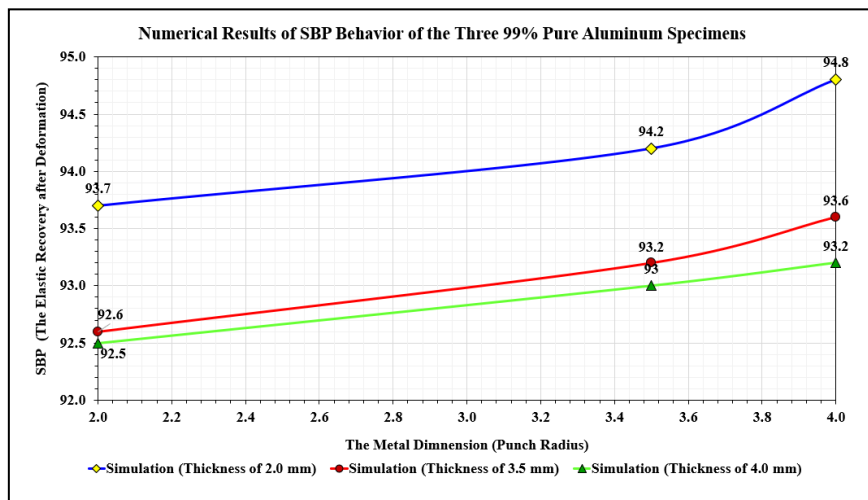

Fig. 9. The behaviour of the SBP from the numerical simulation outcomes of the three 99% pure aluminium specimens (three thicknesses)

Figure 10 shows that the SBP behaviour would decrease slightly with the metal dimension (the punch radius) [28]. Thicker 99% pure copper specimens had better SBP and elastic recovery after deformation than thinner ones. Thus, the 99% pure copper deformation would record greater rates with larger thicknesses but lower values with more punch radius rates [29].

Figure 11 shows that the SBP pattern in the three low-carbon steels rises with greater punch radius values. Low-carbon steel specimens with lower thicknesses exhibit more substantial effects and findings of SBP than those with higher thicknesses.

In conclusion, SBP would greatly affect low-carbon steel specimens with lower thicknesses compared to those with higher thicknesses. Additionally, bigger punch radius rates would produce considerable SBP.
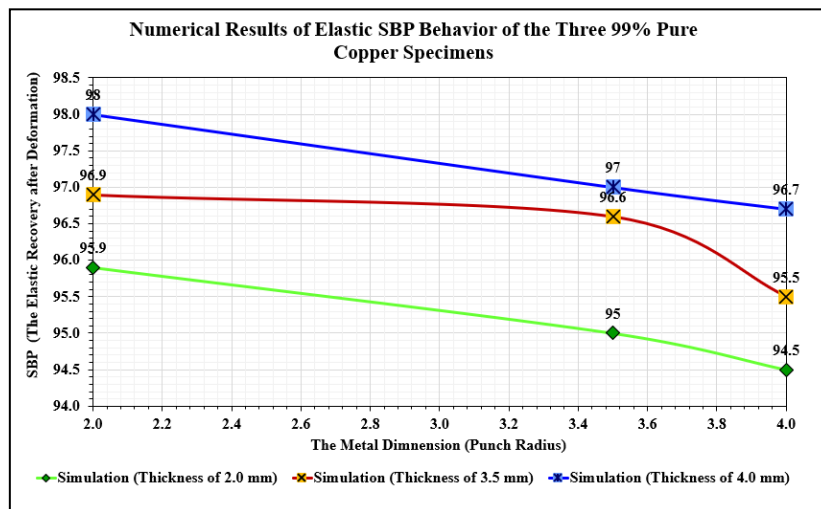
Fig. 10. The behaviour of the SBP from the numerical simulation outcomes of the three 99% pure copper specimens (three thicknesses)
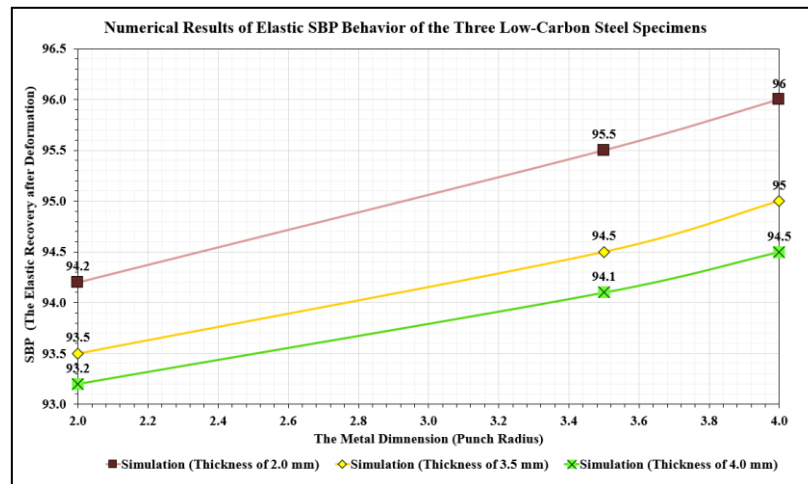

Fig. 11. The behaviour of the SBP from the numerical simulation outcomes of the three 99% low-carbon steel specimens (three thicknesses)

5. HYBRID MODEL INTEGRATION RESULTS ANALYSIS

In the investigation of the metal forming process using hybrid model integration, the three current study metals were selected for numerical analysis. These metals were evaluated based on their mechanical and thermal properties, as well as their behaviour during the forming process. The primary objective of this study was to compare the materials in terms of force, deformation, temperature, equivalent stress distribution, stringback percentage, and material-specific behaviours, in order to identify the most suitable material for various manufacturing applications. The results were obtained through detailed simulations that accounted for the intrinsic properties of the materials, and they provide insights into the overall performance of each material in terms of forming efficiency, quality, and computational demands.

5.1. FORCE AND DEFORMATION

The corresponding outcomes of force, ultimate deformations, and distortion rates obtained from the numerical LS-DYNA ANSYS package simulations revealed distinct differences in the three metals' mechanical and springback behaviours after applying the SMF processes, as can be shown in Fig. 12–14. From Fig. 12, the three specimens of the 99% pure aluminum sheet metal exhibited the lowest peak forming force (of 43 kN, 50 kN, and 52 kN), which is consistent with its lower yield strength compared to 99% pure copper and low-carbon steel. On the other hand, as can be noticed in Fig. 13, the three 99% pure aluminum sheet metal specimens, as expected, showed the highest maximum deformation (of 4.5 mm, 4.2 mm, and 4.7 mm), indicating distortion rates of 4.5%, 4.9%, and 3.2%.

Comparatively, the three sheet metal 99% pure copper specimens, with thicknesses of 2.0 mm, 3.5 mm, and 4.0 mm, exhibited medium rates of the peak bending forces, which equal 75 kN, 73 kN, and 68 kN, respectively. These three specimens, in order, had ultimate deformation proportions of 3.8 mm, 3.5 mm, and 3.6 mm. Responsively, their distortions rates were 3.7%, 4.0%, and 4.1%. In comparison, the three low carbon steel sheet metal samples had peak forming force of 100 kN, 111 kN, and 98 kN, respectively. These three forming forces for the three specimens gave ultimate deformation rates of 2.9 mm, 2.7 mm, and 3.2 mm, in order. These maximum deformation rates corresponded to three distortion percentages of 2.6%, 2.5%, and 2.5%, respectively.
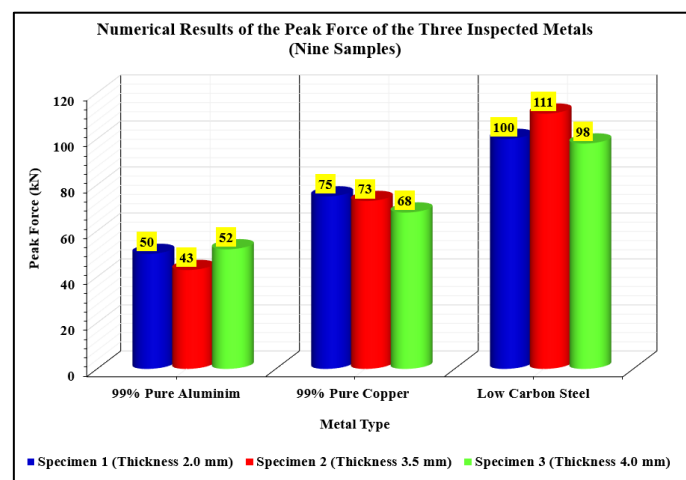

Fig. 12. Simulation outputs of the maximum forming force of the three inspected metals, each with three thicknesses (nine specimens)

In conclusion, it can be inferred from these three figures (Fig. 12–14), that the three aluminum specimens were subjected to the highest deformations (and thus distortions rates) compared to copper and low-carbon steel, because of aluminum's lowest yield strength. Besides, it can be said that because the low-carbon steel has the highest point of yield strength, i.e., being the most robust metal, it can be heavily utilized in a broad scale for lengthy and long SMF processes through which various shapes and forms can be formulated and established, enabling flexible elongation, dimensional stability, and excellent formability before the low carbon steel would reach the failure point (fracture). However, larger

distortions, as will be seen in Fig. 20, do not necessarily imply lower elastic recovery. 99% pure aluminium exhibits the largest elastic recovery compared to the two investigated metals.
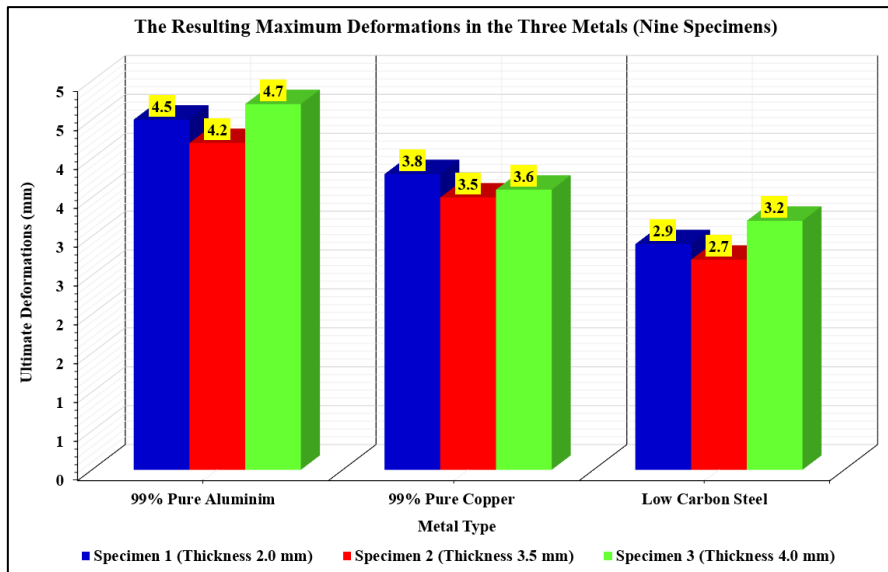

Fig. 13. Simulation outputs of ultimate deformations in the three inspected metals, each with three thicknesses (nine specimens)
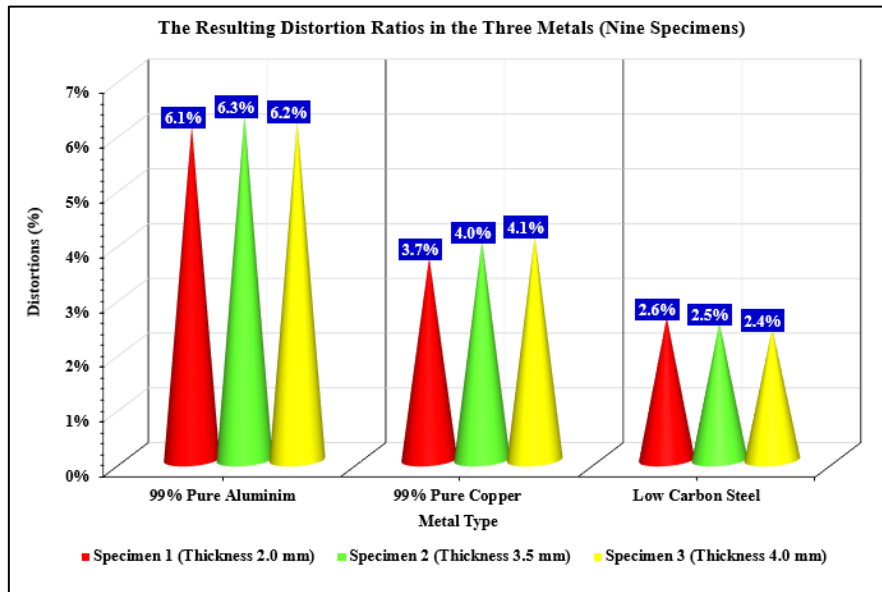

Fig. 14. Simulation outputs of distortion rates in the three inspected metals, each with three thicknesses (nine specimens)

5.2. THE RESULTING VON MISES STRESSES AND EQUIVALENT STRESS CONCENTRATIONS

The numerical LS-DYNA ANSYS package simulations did also supply certain analytical figures on temperature properties, mainly related to the sheet metal's thermal conductivity at the springback occurrence and ultimate exhibited temperature before

deformation would take place. Figure 15 shows the results of the three sheet metals' thermal conductivity at the springback occurrence, each with three thicknesses, which can give nine results.

Furthermore, the equivalent stress distribution outcomes indicate that low-carbon steel had the highest maximum Von Mises stress (420 MPa), as expected due to its higher strength, while 99% pure aluminum experienced lower equivalent stress (280 MPa). 99% of pure copper's Von Mises stress was intermediate, with a maximum of 350 MPa. The equivalent stress concentration in these three metals, shown in Fig. 16, which implies the location at which significantly higher stress amounts are recorded in the metal, was highest in low-carbon steel (451 MPa for a thickness of 4.0 mm), which suggests that while it is a strong material, it is more prone to localized stress accumulation during the forming process. Comparatively, higher equivalent stress concentrations recorded in 99% pure copper and 99% pure aluminum were (382 MPa for a thickness of 3.5 mm) and (311 MPa for a thickness of 4.0 mm), respectively.
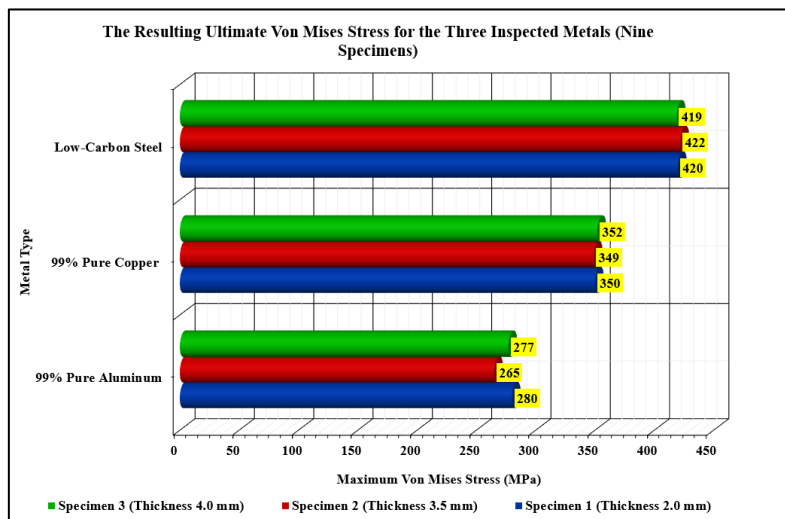

Fig. 15. Simulation outputs of maximum Von Mises stresses in the three inspected metals, each with three thicknesses (nine specimens)
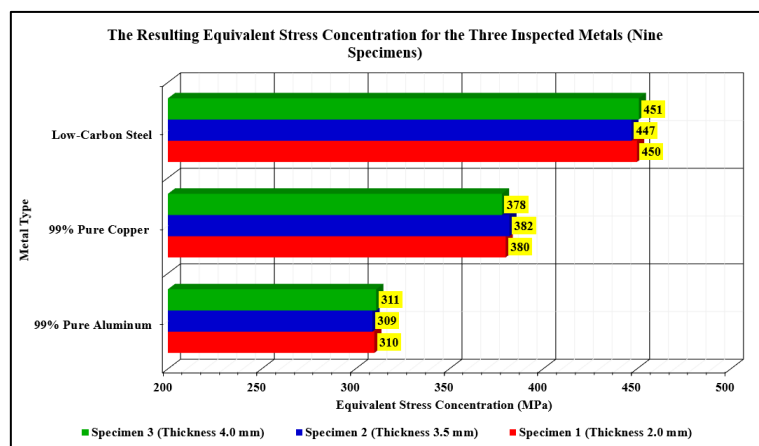

Fig. 16. Simulation outputs of equivalent stress concentrations in the three inspected metals, each with three thicknesses (nine specimens)

5.3. RESULTS OF METALS' THERMAL-RELATED PROPERTIES

One of the imperative outcomes of this research is some corresponding thermal behaviours and properties correlated with the SMF process before deformation takes place and during the SMF. Strictly speaking, it was realized that the three metals did exhibit distinguished ultimate temperature before deformation, as can be clarified in Fig. 17.

It can be inferred from Fig. 17 that the three 99% pure copper specimens, being the best thermally conductive, exhibited the highest rates of ultimate temperature before deformation, specifically 350°, 347°, and 343° for thicknesses of 2.0 mm, 3.5 mm, and 4.0 mm, respectively. In contrast, the three low carbon steel specimens had the lowest ultimate temperature before deformation, reaching 250°, 245°, and 256° for thicknesses 2.0 mm, 3.5 mm, and 4.0 mm, in order. While the three 99% pure aluminium specimens did exhibit a medium range of temperature between the low carbon steel and the 99% pure copper. These statistics can explicitly tell that during the SMF process special considerations should be given to the metal's temperature to prevent adverse impacts on springback ratio (elastic recovery rate) and minimize temperature-related distortions. Additionally, results on the thermal-related properties revealed another index, which is linked to the thermal conductivity documented when the springback phenomenon did take place for the three inspected metals, as can be illustrated in Fig. 18.
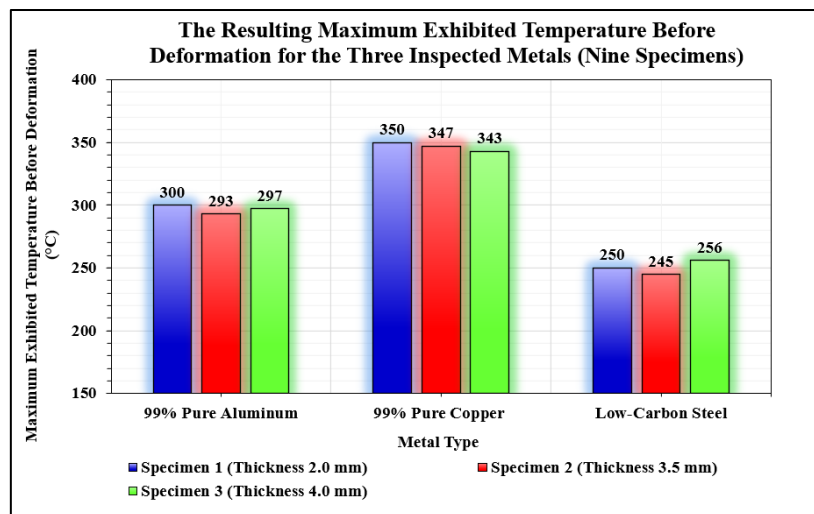

Fig. 17. Simulation outputs of the maximum exhibited temperature before deformation in the three inspected metals, each with three thicknesses (nine specimens)

It can be noted from Fig. 18 that, again, because of its significant, favourable thermal properties among other metals in nature, the three 99% pure copper specimens exhibited the maximum rates of thermal conductivity, recording 398 W/m.K, 399 W/m.K, and 400 W/m.K for thicknesses 2.0 mm, 3.5 mm, and 4.0 mm, respectively, when the springback phenomenon did occur. Comparatively, the three low carbon steel specimens had the lowest thermal conductivity during the springback behaviour, revealing thermal conductivities of 79 W/m.K, 80 W/m.K, and 81 W/m.K for thicknesses 2.0 mm, 3.5 mm, and 4.0 mm, in order, throughout springback.

These ANSYS outcomes of thermal-related properties can explain that, because of the lowest thermal conductivity during the SMF process and very low temperature at springback, the low carbon steel can be remarkably resistant to heat transfer and thermal-related changes when necessary SMF processes are performed. Thus, the low carbon steel can give substantial flexibility in SMF and formability without being adversely affected by critical thermal properties.
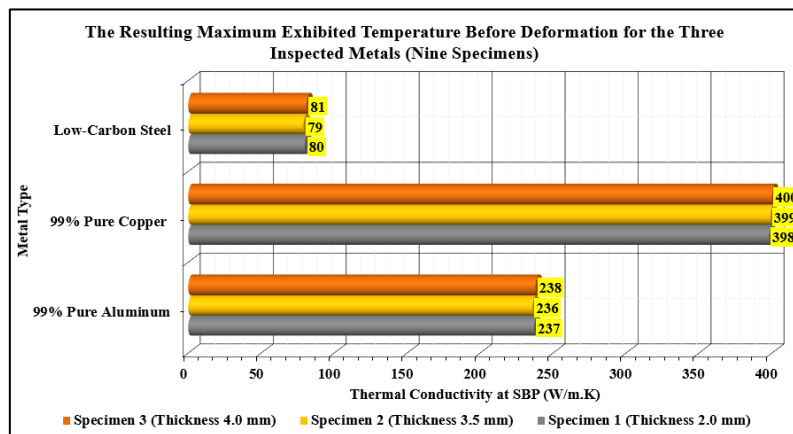

Fig. 18. Simulation outputs of the thermal conductivity at the springback phenomenon in the three inspected metals, each with three thicknesses (nine specimens)

5.4. THE RESULTING METALS' SPRINGBACK ANGLE AND SHAPE DEVIATION

The springback and post-processing behaviour simulation outcomes emphasized how each metal would behave once the forming force is removed, as can be shown in Fig. 19. The three 99% pure aluminum sheet metals showed the largest springback bending angles of 4.5°, 4.3°, and 4.4° for the thicknesses 2.0 mm, 3.5 mm, and 4.0 mm, respectively, implying aluminum's higher elasticity and tendency to return to their original shapes after deformation.
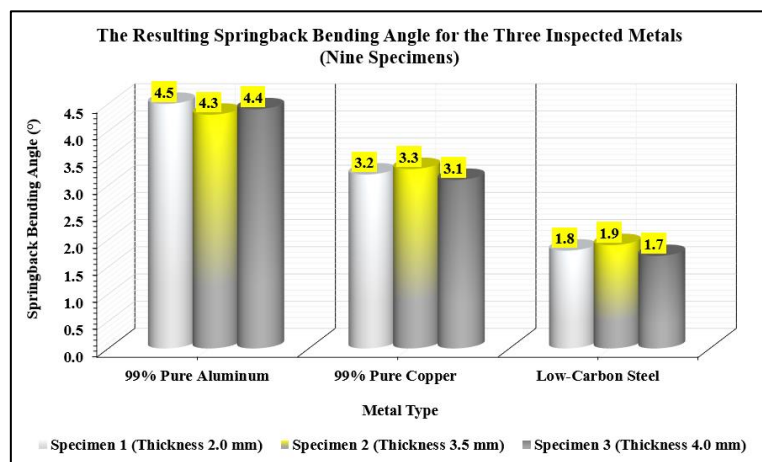

Fig. 19. Simulation outputs of springback bending angle in the three inspected metals, each with three thicknesses (nine specimens)

The three 99% pure copper sheet metal samples, in comparison, had springback bending angles of 3.2°, 3.3°, and 3.1° for the thicknesses 2.0 mm, 3.5 mm, and 4.0 mm, respectively, exhibiting moderate recovery. While the three low-carbon steel sheet metal specimens showed the least values of springback bending angles of 1.8°,1.9°, and 1.7° for the three thicknesses 2.0 mm, 3.5 mm, and 4.0 mm, reflecting low carbon steel's reduced ability to return to its original shape. The final shape deviation was also evaluated, with 99% pure aluminum showing the largest deviation (2.2 mm), followed by 99% pure copper (1.7 mm) and low-carbon steel (0.9 mm). This suggests that in spite of 99% pure aluminum's higher formability, it may face less precision to be formulated to the final needed shapes compared to 99% pure copper and low-carbon steel.

5.5. MATERIAL-RELATED PROPERTIES

The material-specific behaviour analysis was conducted, and its corresponding outcomes can be shown in Table (4).

Table 4. The Resulting Material-specific behaviour attained from the ANSYS LS-DYNA

#	Material	Yield Strength (MPa)	Elongation at Break (%)	Ductility
1	99% Pure Aluminum	250	25	High
2	99% Pure Copper	210	35	Very High
3	Low-Carbon Steel	350	15	Low

These outcomes have been obtained through a systematic analytical procedure. To investigate Table 4's variables of each metal, namely the yield point, elongation at break, and ductility, elastic-plastic material models were chosen in the LS-DYNA ANSYS package. Loads and boundary conditions were then applied. The punch force or displacement were then identified. Symmetric constraints were then applied to reduce computational cost, time, and technical complexity. Adaptive meshing was utilized to improve accuracy in high-deformation regions. Then, simulation process was conducted by running numerical analysis, solving the SMF process. Before unloading, the deformation history of the metal was recorded and investigated as historical deformations of each metal may have considerable impact on the yield stress, Von Misses stress, elastic strain, and deformations. Then, the unloading process was simulated in the LS-DYNA ANSYS package. After that, the punch force was gradually removed to enable the metal to springback. After that, the software provided some data on the residual stress and final geometry. Also, the attained results gave important insights on the springback.

A comparison, in this respect, should be performed in terms of the final and needed shape to uncover to which extent springback (elastic recovery ratio) would take place, enabling the metal to return to its original shape after removing the load. Figure 20 indicates this comparative analysis.

It can be noticed from this table that 99% pure copper is the most ductile material, with a high elongation at break of 35% and superior overall ductility. 99% pure aluminum, while still relatively ductile, had a lower elongation at break (25%), and low-carbon steel had the

lowest ductility with only 15% elongation at break. Yield strength was highest in low-carbon steel (350 MPa), followed by 99% pure aluminum (250 MPa), and 99% pure copper (210 MPa). These results are consistent with the general understanding that low-carbon steel is stronger but less ductile than 99% pure aluminum and 99% pure copper.
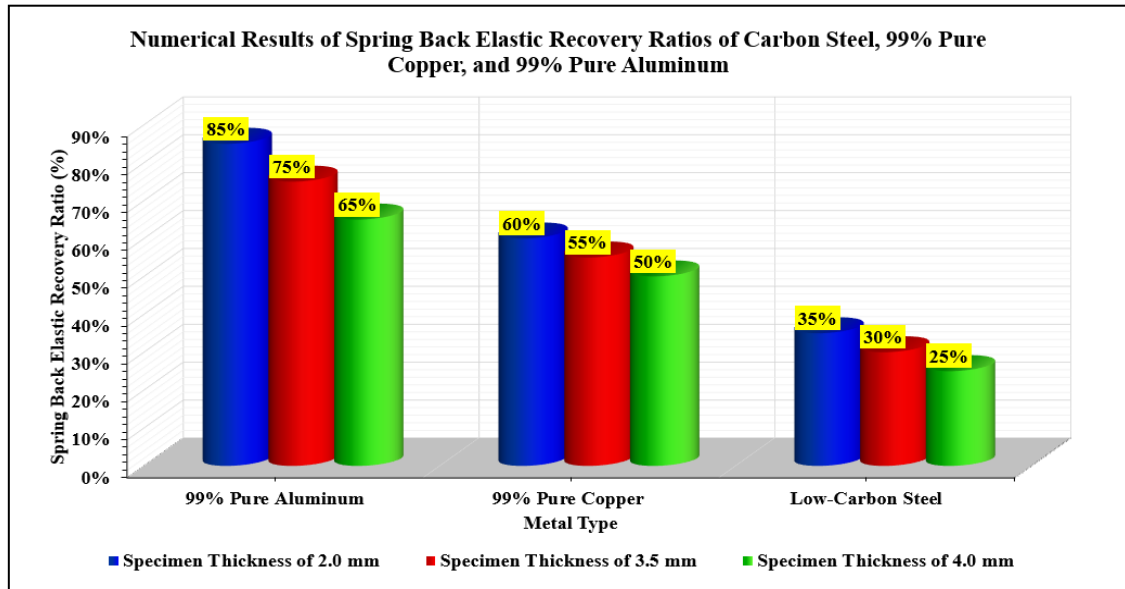

Fig. 20. Numerical simulation outputs of springback elastic recovery percentage of the three investigated metals, each with sheet metal thicknesses of 2.0 mm, 3.5 mm, and 4.0 mm

5.6. THE RESULTING COMPUTATIONAL PERFORMANCE

The computational performance analysis indicated the time and mesh size required for each material during the simulation process, as can be shown in Table (5). As expected, the simulation time would increase in metals with higher yield strength, enhanced mechanical properties, remarkably significant stiffness, larger modulus of elasticity, and robust durability. In this respect, among the three metals, low-carbon steel required the longest time (5 hours) due to its larger mesh size (250,000 elements) and promoted springback resilience and resistance behaviour. 99% pure copper and 99% pure aluminum, with smaller mesh sizes (200,000 and 150,000 elements respectively), required less time, but 99% pure copper still took more time than 99% pure aluminum due to its more complicated equivalent stress and temperature distribution. Solver efficiency decreased slightly with the increasing number of elements, but the hybrid model remained efficient for industrial applications despite the increased computational demand for more complex materials.

Table 5. Computational performance

#	Material	Simulation Time (hrs)	Mesh Size (Elements)	Solver Efficiency
1	99% Pure Aluminum	3.5	150,000	85%
2	99% Pure Copper	4.0	200,000	80%
3	Low-Carbon Steel	5.0	250,000	75%

In summary, each material, 99% pure aluminum, 99% pure copper, and low-carbon steel, demonstrated unique advantages and limitations in terms of forming force, deformation, equivalent stress distribution, and post-processing behaviour. These findings provide critical insights for selecting the appropriate material based on specific forming requirements, whether it be ease of shaping (99% pure aluminum), superior ductility (99% pure copper), or higher strength (low-carbon steel).

5.7. COMPARATIVE ANALYSIS OF THE SBP BETWEEN THE THREE METALS

To provide a better understanding of how each metal has responded to the die loading and the resulting SBP elastic recovery, the elastic recovery ratios of the three metals at different thicknesses (2.0 mm, 3.5 mm, and 4.0 mm) are now expressed in percentage terms. It is imperative to clarify that a distortion rate of 8% does not mean an elastic recovery (springback percentage) of 92%, since there are some factors that can cause losses, including interior elasticity of the metal. In nature, all metals are not fully elastic, meaning that elastic recovery of 92% does not mean necessarily a distortion percentage of 8%.

This allows for a more quantifiable comparison of how each material behaves under the applied loads. The results of the SBP behaviour for each metal at different thicknesses are shown in Fig. 20.

The elastic recovery ratios for the three metals at different thicknesses demonstrate varying levels of springback behaviour. At a thickness of 2.0 mm, the 99% pure aluminum sheet metal exhibits the highest elastic recovery ratio of 85%, showing that it responds well to die loading and recovers most of its shape after deformation. 99% pure copper follows a moderate recovery of 60%, while low-carbon steel shows the lowest recovery at 35%, indicating significant deformation that does not fully recover after the die loading.

For a thickness of 3.5 mm, 99% pure aluminum still maintains the highest springback at 75%, but this is a decrease from its performance at 2.0 mm. 99% pure copper's recovery ratio decreases to 55%, and low-carbon steel continues to show the lowest recovery at 30%, further emphasizing its poor performance in terms of elastic recovery.

At 4.0 mm thickness, the springback behaviour of 99% pure aluminum is again reduced to 65%, while 99% pure copper experiences a slight decrease to 50%. Low-carbon steel still has the lowest elastic recovery at 25%, confirming that it exhibits the least ability to recover from die loading among the three metals. This analysis can imply that 99% pure aluminum can consistently perform the best in terms of springback across all thicknesses, while low-carbon steel exhibits the poorest elastic recovery, especially as the thickness increases. 99% pure copper exists between the two, with moderate springback across the three thicknesses.

6. CONCLUSIONS

This study explored the critical contributions and practicality of a hybrid advanced FEA-ML framework to predict the springback phenomenon (SBP) in metals. To provide reliable validity and robustness of the research outcomes, the most prevalent metals utilized in the

manufacturing context of many critical disciplines, like automotive, aircraft, and ship structuring, have been investigated, namely low-carbon steel, 99% pure aluminum, and 99% pure copper. Reliable mathematical simulations and numerical analysis were conducted in the LS-DYNA ANSYS package. To introduce the impacts of SBP, a collection of common variables and imperative factors have been inspected, namely punch radius, angle of SBP, temperature effects, metal's thickness, and some other crucial indices, which have considerable influence on the behaviour of these three metals when SBP takes place.

Relying on the systematic research methodology that was adopted in this study, the major research outcomes can be summarized in the following points:

- Springback behaviour varied significantly among the three metals, with 99% pure aluminum exhibiting the highest elastic recovery and springback (6.2%) due to its high ductility, followed by 99% pure copper (4.0%), and low-carbon steel (2.5%),
- Low-carbon steel showed the least elastic recovery behaviour and lowest springback pattern, indicating its suitability for applications requiring precise dimensional control post-forming before metal failure. At a thickness of 2.0 mm in the three metals, 99% pure aluminum required the lowest peak forming force (50 kN) and showed the highest deformation rates (4.5 mm), implying its considerable flexibility as a formable material. 99% pure copper required a higher forming force (75 kN) with moderate deformation (3.8 mm), while low-carbon steel, being the strongest material, exhibited the highest forming force (100 kN) and the least deformation (2.9 mm),
- 99% pure copper experienced the highest temperature rise (350 °C) during the SMFP due to its superior thermal conductivity, followed by the 99% pure aluminum (300 °C) and low-carbon steel (250 °C),
- Thinner specimens exhibited more pronounced springback effects across all three metals, while increased punch radii enhanced the springback behaviour,
- 99% pure copper had the highest ductility (35% elongation at break), making it ideal for applications requiring significant deformation without failure. Aluminum exhibited good ductility (25% elongation) and high formability but showed larger shape deviations post-forming. Low-carbon steel, with the highest yield strength (350 MPa) and lowest elongation (15%), provided excellent strength and dimensional stability but reduced malleability,
- The advanced hybrid FEA-ML framework proved its significant effectiveness, reliability, accuracy, and efficiency in predicting springback angles, reducing reliance on time-intensive experiments that correspond to many faults and optimizing the metal forming process.

Besides these findings, a conclusion can be reached that 99% pure aluminum is suitable for lightweight applications, like the automotive domain, while low-carbon steel is preferred in scenarios requiring high strength and dimensional stability. Copper, with its balance of ductility and strength, is well-suited for intricate forming processes. Finally, this hybrid approach can offer a promising tool for optimizing manufacturing processes, improving product quality, and enhancing efficiency across various engineering sectors. In this respect, possible future research could expand the applicability of this model to more complex geometries and multi-metal systems, further advancing the field of metal-forming technology.

REFERENCES

[1] MEDA D.P., 2020, *Modeling And Experimental Investigation of Springback in Brass Alloy Sheet Metal V-Bending*, Master's thesis, Eastern Mediterranean University (EMU)-Doğu Akdeniz Üniversitesi (DAÜ).

[2] ATTAR H.R., ZHU L., LI N., 2023 *Check for Updates Deep Learning Enabled Tool Compensation for Addressing Shape Distortion in Sheet Metal Stamping*, In Proceedings of the 14th International Conference on the Technology of Plasticity-Current Trends in the Technology of Plasticity, 4, 48.

[3] BOLAR A.L., 2023, *Automation of a Multi-Stage T-Joint Assembly of Stamped Components and Prediction of Performance Parameters Using Machine Learning*, Master's thesis, The Ohio State University.

[4] WANG Z., XIANG Y., ZHANG S., LIU X., MA J., TAN J., WANG L., 2024, *Physics-Informed Springback Prediction of 3D Aircraft Tubes with Six-Axis Free-Bending Manufacturing*, Aerospace Science and Technology, 147, 109022.

[5] ETIM B., AL-GHOSOUN A., RENNO J., SEAID M., MOHAMED M.S., 2024, *Machine Learning-Based Modelling for Structural Engineering: A Comprehensive Survey and Applications Overview,* Buildings, 14/11, 3515.

[6] XU J., 2022, *Machine Learning Applications for Studying the Structural Behaviour of Cold-Formed Steel Columns with Web Openings ,*Doctoral dissertation, Research Space@ Auckland.

[7] HE J., CU S., XIA H., SUN Y., XIAO W., REN Y., 2023, *High Accuracy Roll Forming Springback Prediction Model of SVR Based on SA-PSO Optimization*, Journal of Intelligent Manufacturing, 36, 167–183.

[8] ZEINOLABEDIN-BEYGI A., NAEINI H.M., TALEBI-GHADIKOLAEE H., RABIEE A.H., HAJIAHMADI S., 2024, *Predictive Modelling of Spring-Back in Pre-Punched Sheet Roll Forming Using Machine Learning,* The Journal of Strain Analysis for Engineering Design, 59/7, 463–474.

[9] SAFARI M., RABIEE A.H., JOUDAKI J., 2023, *Developing a Support Vector Regression (SVR) Model for Prediction of Main and Lateral Bending Angles in Laser Tube Bending Process*, Materials, 16/8, 3251.

[10] LEI C., MAO J., ZHANG X., WANG L., CHEN D., 2021, *Crack Prediction in Sheet Forming of Zirconium Alloys Used in Nuclear Fuel Assembly by Support Vector Machine Method*, Energy Reports, 7, 5922–5932.

[11] FENG Y., HONG Z., GAO Y., LU R., WANG Y., TAN J., 2019, *Optimization of Variable Blank Holder Force in Deep Drawing Based on Support Vector Regression Model and Trust Region*, The International Journal of Advanced Manufacturing Technology, 105, 4265–4278.

[12] WANG H., CHEN L., YE F., WANG J., 2018, *A Multi-Hierarchical Successive Optimization Method for Reduction of Spring-Back in Autoclave Forming*, Composite Structures, 188, 143–158.

[13] CINAR Z., ASMAEL M., ZEESHAN Q., SAFAEI B., 2021, *Effect of Springback on A6061 Sheet Metal Bending: A Review*, Journal Kejuruteraan, 33/1, 13–26.

[14] YUE Z., QI J., ZHAO X., BADREDDINE H., GAO J., CHU X., 2018, *Springback Prediction of Aluminum Alloy Sheet Under Changing Loading Paths with Consideration of the Influence of Kinematic Hardening and Ductile Damage*, Metals, 8/11, 950.

[15] TSENG A.A., JEN K.P., CHEN T.C., KONDETIMMAMHALLI R., MURTY Y.V., 1995, *Forming Properties and Springback Evaluation of Copper Beryllium Sheets*, Metallurgical and Materials Transactions A, 26, 2111–2121.

[16] PANDIT A., DAS S., DAS S.K., 2020, *Investigation on Spring-Back Effect of Galvanized Iron Sheet*, Reason-A Technical Journal, 81–93, https://doi.org/10.21843/reas/2020/81-93/209274.

[17] ADAY A.J., 2019, *Analysis of Springback Behaviour in Steel and Aluminum Sheets Using FEM*, Ann. de Chim. Sci. des Materiaux, 43/2, 95–98.

[18] TEJYAN S., KUMAR N., RAVI R.K., SINGH V., GANGIL B., 2024, *Analysis of Spring Back Effect for AA6061 Alloy Sheet Using Finite Element Analysis*, Materials Today: Proceedings, https://doi.org/10.1016/j.matpr.2024.05.122.

[19] WANG X.Z., MASOOD S.H., NG D., DAWWAS O., 2011, *A Study of Springback of Sheet Metal Formed Parts Using ANSYS*, Advanced Materials Research, 291, 381–384.

[20] ZHANG Z., ZHENG C., LIU J., ZHONG Y., 2024, *Springback Research of Tubular Structure Under Lateral Compression Using Explicit and Implicit FEA Method*, Journal of Physics, Conference Series, 2820, 1, 012061.

[21] ABDULHASAN M.Q., 2019, *Design of Flexible Tool for the Evaluation of Plate Springback*, Doctoral dissertation, Ministry of Higher Education, Al-Nahrain University, https://doi.org/10.13140/RG.2.2.36133.37604.

[22] JOSEPH C.D., 2003, *Experimental Measurement and Finite Element Simulation of Springback in Stamping Aluminum Alloy Sheets for Auto-Body Panel Application*, Mississippi State University, Engineering, Materials Science, Corpus ID: 5980229.

[23] PRAKASH S., ETHIER C.R., 2001, *Requirements for Mesh Resolution in 3D Computational Hemodynamics*, J. Biomech. Eng., 123/2, 134–144.

[24] ADRIAN A.F., 2022, *Automation and Validation of Big Data Generation via Simulation Pipeline for Flexible Assemblies*, Master's thesis, The Ohio State University.

[25] DEZELAK M., PAHOLE I., FICKO M., BREZOCNIK M., 2012, *Machine Learning for the Improvement of Springback Modelling*, Advances in Production Engineering & Management, 7/1,17–26, https://doi.org/10.14743/apem2012.1.127.

[26] JAMLI M.R., FARID N.M., 2019, *The Sustainability of Neural Network Applications Within Finite Element Analysis in Sheet Metal Forming: A Review*, Measurement, 138, 446–460.

[27] KUMAR P., 2024, *A Study on the Extraction of Geometrical Parameters from Flexible Mechanical Components and Assemblies and Their Impact on Performance: a Machine Learning Approach*, Master's thesis, Arizona State University.

[28] ABDULLAH E., JALIL A., 2024, *Critical Spring Back Characteristics in Aluminum, Copper, and Pure Steel*: *Experimental Analysis*, Proc. IMechE Part B, J. Engineering Manufacture, 231/4, 675–689.

[29] CHANDRASEKARAN P., MANONMANI K., 2015, *A Review on Springback Effect in Sheet Metal Forming Process*, Int. Conf. Syst. Sci. Control Commun. Eng. Technol., 43–49, Engineering, Materials Science, Corpus ID: 51691117.